

MODEL-INDEPENDENT CONSTRAINTS ON DARK ENERGY DENSITY FROM FLUX-AVERAGING ANALYSIS OF TYPE IA SUPERNOVA DATA

YUN WANG¹, AND PIA MUKHERJEE¹
Draft version November 14, 2018

ABSTRACT

We reconstruct the dark energy density $\rho_X(z)$ as a free function from current type Ia supernova (SN Ia) data (Tonry et al. 2003; Barris et al. 2003; Knop et al. 2003), together with the Cosmic Microwave Background (CMB) shift parameter from CMB data (WMAP, CBI, and ACBAR), and the large scale structure (LSS) growth factor from 2dF galaxy survey data. We parametrize $\rho_X(z)$ as a continuous function, given by interpolating its amplitudes at equally spaced z values in the redshift range covered by SN Ia data, and a constant at larger z (where $\rho_X(z)$ is only weakly constrained by CMB data). We assume a flat universe, and use the Markov Chain Monte Carlo (MCMC) technique in our analysis. We find that the dark energy density $\rho_X(z)$ is constant for $0 \lesssim z \lesssim 0.5$ and increases with redshift z for $0.5 \lesssim z \lesssim 1$ at 68.3% confidence level, but is consistent with a constant at 95% confidence level. For comparison, we also give constraints on a constant equation of state for the dark energy.

Flux-averaging of SN Ia data is required to yield cosmological parameter constraints that are free of the bias induced by weak gravitational lensing (Wang 2000b). We set up a consistent framework for flux-averaging analysis of SN Ia data, based on Wang (2000b). We find that flux-averaging of SN Ia data leads to slightly lower Ω_m and smaller time-variation in $\rho_X(z)$. This suggests that a significant increase in the number of SNe Ia from deep SN surveys on a dedicated telescope (Wang 2000a) is needed to place a robust constraint on the time-dependence of the dark energy density.

Subject headings: cosmology:observations – distance scale – supernovae:general

1. INTRODUCTION

Observational data of type Ia supernovae (SNe Ia) indicate that our universe is dominated by dark energy today (Riess et al. 1998; Perlmutter et al. 1999). The nature of dark energy is one of the great mysteries in cosmology at present. The time-dependence of the dark energy density $\rho_X(z)$ can illuminate the nature of dark energy, and help differentiate among the various dark energy models (for example, Freese et al. (1987); Peebles & Ratra (1988); Frieman et al. (1995); Caldwell, Dave, & Steinhardt (1998); Dodelson, Kaplinghat, & Stewart (2000); Deffayet (2001); Albrecht et al. (2002); Boyle, Caldwell, & Kamionkowski (2002); Freese & Lewis (2002); Griest (2002); Sahni & Shtanov (2002); Carroll, Hoffman, & Trodden (2003); Farfar & Peebles (2003). See Padmanabhan (2003) and Peebles & Ratra (2003) for reviews with more complete lists of references).

SNe Ia can be calibrated to be good cosmological standard candles, with small dispersions in their peak luminosity (Phillips 1993; Riess, Press, & Kirshner 1995). The measurements of the distance-redshift relations of SNe Ia are most promising for constraining the time variation of the dark energy density $\rho_X(z)$. The luminosity distance $d_L(z) = (1+z)r(z)$, with the comoving distance $r(z)$ given by

$$r(z) = cH_0^{-1} \int_0^z \frac{dz'}{E(z')}, \quad (1)$$

where

$$E(z) \equiv [\Omega_m(1+z)^3 + \Omega_k(1+z)^2 + \Omega_X \rho_X(z)/\rho_X(0)]^{1/2}, \quad (2)$$

with $\Omega_k \equiv 1 - \Omega_m - \Omega_X$. If the dark energy equation of

state $w_X(z) = w_0 + w_1 z$, then

$$\frac{\rho_X(z)}{\rho_X(0)} = e^{3w_1 z} (1+z)^{3(1+w_0-w_1)}. \quad (3)$$

The dark energy density $\rho_X(z) = \rho_X(0)(1+z)^{3(1+w_0)}$ if the dark energy equation of state is a constant given by w_0 .

Most researchers have chosen to study dark energy by constraining the dark energy equation of state w_X . However, due to the smearing effect (Maor, Brustein, & Steinhardt 2001) arising from the multiple integrals relating $w_X(z)$ to the luminosity distance of SNe Ia, $d_L(z)$, it is extremely hard to constrain w_X using SN data without making specific assumptions about w_X (Barger & Marfattia 2001; Huterer & Turner 2001; Maor et al. 2002; Wasserman 2002). If we constrain the dark energy density $\rho_X(z)$ instead, we minimize the smearing effect by removing one integral (Wang & Garnavich 2001; Tegmark 2002; Daly & Djorgovski 2003).

It is important that there are a number of other probes of dark energy that are complementary to SN Ia data (for example, see Podariu & Ratra (2001); Schulz & White (2001); Bean & Melchiorri (2002); Hu (2002); Sereno (2002); Bernstein & Jain (2003); Huterer & Ma (2003); Jimenez (2003); Majumdar & Mohr (2003); Mukherjee et al. (2003); Munshi & Wang (2003); Munshi, Porciani, & Wang (2003); Seo & Eisenstein (2003); Viel et al. (2003); Weller & Lewis (2003); Zhu & Fujimoto (2003)). Since different methods differ in systematic uncertainties, the comparison of them will allow for consistency checks, while the combination of them could yield tighter constraints on dark energy (for example, see Gerke & Efstathiou (2002); Hannestad & Mortsell (2002); Kujat et al. (2002)).

¹ Department of Physics & Astronomy, Univ. of Oklahoma, 440 W Brooks St., Norman, OK 73019; email: wang,pia@nhn.ou.edu

The most pressing question about dark energy that can be addressed by observational data is whether the dark energy density varies with time. In order to constrain the time-variation of dark energy density in a robust manner, it is important that we allow the dark energy density to be an arbitrary function of redshift z (Wang & Garnavich 2001; Wang & Lovelace 2001; Wang et al. 2003). In this paper, we present a model-independent reconstruction of the dark energy density $\rho_X(z)$, using SN Ia data published recently by the High- z Supernova Search Team (HST) and the Supernova Cosmology Project (SCP) (Tonry et al. 2003; Barris et al. 2003; Knop et al. 2003), together with constraints from CMB (WMAP (Bennett et al. 2003), CBI (Pearson et al. 2003), and ACBAR (Kuo et al. 2002)) and large scale structure (LSS) data from the 2dF galaxy survey (Percival et al. 2002).

Note that for clarity of presentation, we will label the samples of SNe Ia that we use according to the papers in which they were published. Hence we will refer to the 194 SNe Ia from Tonry et al. (2003) and Barris et al. (2003) as the ‘‘Tonry/Barris sample’’, and the 58 SNe Ia from Knop et al. (2003) as the ‘‘Knop sample’’.

Flux-averaging of SN Ia data is required to yield cosmological parameter constraints that are free of the bias induced by weak gravitational lensing (Wang 2000b). In this paper, we set up a consistent framework for flux-averaging analysis of SN Ia data, based on Wang (2000b).

We assume a flat universe, and use the Markov Chain Monte Carlo (MCMC) technique in our analysis.

Sec.2 contains a consistent framework for flux-averaging analysis. We present our constraints on dark energy in Sec.3. Sec.4 contains a summary and discussions.

2. A CONSISTENT FRAMEWORK FOR FLUX-AVERAGING ANALYSIS

Since our universe is inhomogeneous in matter distribution, weak gravitational lensing by galaxies is one of the main systematics² in the use of SNe Ia as cosmological standard candles (Kantowski, Vaughan, & Branch 1995; Frieman 1997; Wambsganss et al. 1997; Holz & Wald 1998; Metcalf & Silk 1999; Wang 1999; Wang, Holz, & Munshi 2002; Munshi & Wang 2003). Flux-averaging *justifies* the use of the distance-redshift relation for a smooth universe in the analysis of type Ia supernova (SN Ia) data (Wang 2000b). Flux-averaging of SN Ia data is required to yield cosmological parameter constraints that are free of the bias induced by weak gravitational lensing (Wang 2000b).³ Here we set up a consistent framework for flux-averaging analysis of SN Ia data, based on Wang (2000b).

2.1. Why flux-averaging?

The reason that flux-averaging can remove/reduce gravitational lensing bias is that due to flux conservation, the average magnification of a sufficient number of standard candles at the same redshift is one.

The observed flux from a SN Ia can be written as

$$F(z) = F_{int} \mu, \quad F_{int} = F^{tr}(z|\mathbf{s}^{tr}) + \Delta F_{int}, \quad (4)$$

where $F^{tr}(z|\mathbf{s}^{tr})$ is the predicted flux due to the true cosmological model parametrized by the set of cosmological parameters $\{\mathbf{s}^{tr}\}$, ΔF_{int} is the uncertainty in SN Ia peak brightness due to intrinsic variations in SN Ia peak luminosity and observational uncertainties, and μ is the magnification due to gravitational lensing by intervening matter. Therefore

$$\Delta F^2 = \mu^2 (\Delta F_{int})^2 + (F_{int})^2 (\Delta \mu)^2. \quad (5)$$

Without flux-averaging, we have

$$\begin{aligned} \chi_{N_{data}}^2(\mathbf{s}^{tr}) &= \sum_i \frac{[F(z_i) - F^{tr}(z_i|\mathbf{s}^{tr})]^2}{\sigma_{F,i}^2} \\ &= \sum_i \frac{[F^{tr}(z_i)(\mu_i - 1)]^2 + \mu_i^2 [\Delta F_{int}^{(i)}]^2}{\sigma_{F,i}^2} + \\ &\quad 2 \sum_i \frac{F^{tr}(z_i) \Delta F_{int}^{(i)} \mu_i (\mu_i - 1)}{\sigma_{F,i}^2} \\ &= N_{data} + 2 \sum_i \frac{F^{tr}(z_i) \Delta F_{int}^{(i)} \mu_i (\mu_i - 1)}{\sigma_{F,i}^2}. \end{aligned} \quad (6)$$

The flux-averaging described in the Section 2.3 leads to the flux in each redshift bin

$$\bar{F}(\bar{z}_{i_{bin}}) = F^{tr}(\bar{z}_{i_{bin}}) \langle \mu \rangle_{i_{bin}} + \langle \mu \Delta F_{int} \rangle_{i_{bin}}. \quad (7)$$

For a sufficiently large number of SNe Ia in the i -th bin, $\langle \mu \rangle_{i_{bin}} = 1$. Hence

$$\chi_{N_{bin}}^2(\mathbf{s}^{tr}) \simeq \sum_{i_{bin}}^{N_{bin}} \frac{[\langle \mu \Delta F_{int} \rangle_{i_{bin}}]^2}{\sigma_{F,i_{bin}}^2} \simeq \sum_{i_{bin}}^{N_{bin}} \frac{[\langle \Delta F_{int} \rangle_{i_{bin}}]^2}{\sigma_{F,i_{bin}}^2} < N_{bin}. \quad (8)$$

Comparison of Eq.(8) and Eq.(6) shows that flux-averaging can remove/reduce the gravitational lensing effect, and leads to a smaller χ^2 per degree of freedom for the true model, compared to that from without flux-averaging.

2.2. Flux statistics versus magnitude statistics

Normally distributed measurement errors are required if the χ^2 parameter estimate is to be a maximum likelihood estimator (Press et al. 1994). Hence, it is important that we use the χ^2 statistics with an observable that has a error distribution closest to Gaussian.

So far, it has been assumed that the distribution of observed SN Ia peak brightness is Gaussian in *magnitudes*. Therefore, for a given set of cosmological parameters $\{\mathbf{s}\}$

$$\chi^2 = \sum_i \frac{[\mu_0(z_i) - \mu_0^p(z_i|\mathbf{s})]^2}{\sigma_{\mu_0}^2}, \quad (9)$$

where $\mu_0^p(z) = 5 \log(d_L(z)/\text{Mpc}) + 25$, and $d_L(z) = (1+z)r(z)$ is the luminosity distance.

However, while we do not have a very clear understanding of how the intrinsic dispersions in SN Ia peak luminosity is distributed, the distribution of observational uncertainties in SN Ia peak brightness is Gaussian in *flux*, since CCD's have replaced photometric plates as detectors of photons.

² The others systematics are possible gray dust (Aguirre 1999) and SN Ia peak luminosity evolution (Drell, Loredo, & Wasserman 2000; Riess et al. 1999; Wang 2000b); so far, there is no clear evidence of either.

³ To avoid missing the faint end (which is fortunately steep) of the magnification distribution of observed SNe Ia, only SNe Ia detected well above the threshold should be used in flux-averaging.

In this paper, we assume that the intrinsic dispersions in SN Ia peak brightness is Gaussian in *flux*, and not in magnitude as assumed in all previous publications. The justifications for this preference will be presented in detail elsewhere (Wang et al. 2004)⁴. Thus,

$$\chi_{N_{data}}^2(\mathbf{s}) = \sum_i \frac{[F(z_i) - F^p(z_i|\mathbf{s})]^2}{\sigma_{F,i}^2}. \quad (10)$$

Since the peak brightness of SNe Ia have been given in magnitudes with symmetric error bars, $m_{peak} \pm \sigma_m$, we obtain equivalent errors in flux as follows:

$$\sigma_F \equiv \frac{F(m_{peak} + \sigma_m) - F(m_{peak} - \sigma_m)}{2} \quad (11)$$

We will refer to Eq.(9) as “magnitude statistics”, and Eq.(10) as “flux statistics”. For reference and comparison, we present results in both “magnitude statistics” and “flux statistics” in this paper. However, a consistent framework for flux-averaging is only straightforward in “flux statistics”.⁵

2.3. A recipe for flux-averaging

The procedure for flux-averaging in Wang (2000b) is for minimizing χ^2 using the subroutines from Numerical Recipes (Press et al. 1994). As described in Wang (2000b), the fluxes of SNe Ia in a redshift bin should only be averaged *after* removing their redshift dependence, which is a model-dependent process. For χ^2 statistics using MCMC or a grid of parameters, here are the steps in flux-averaging:

(1) Convert the distance modulus of SNe Ia into “fluxes”,

$$F(z_j) \equiv 10^{-(\mu_0(z_j) - 25)/2.5} = \left(\frac{d_L^{data}(z_j)}{\text{Mpc}} \right)^{-2}. \quad (12)$$

(2) For a given set of cosmological parameters $\{\mathbf{s}\}$, obtain “absolute luminosities”, $\{\mathcal{L}(z_j)\}$, by removing the redshift dependence of the “fluxes”, i.e.,

$$\mathcal{L}(z_j) \equiv d_L^2(z_j|\mathbf{s}) F(z_j). \quad (13)$$

(3) Flux-average the “absolute luminosities” $\{\mathcal{L}_j^i\}$ in each redshift bin i to obtain $\{\bar{\mathcal{L}}^i\}$:

$$\bar{\mathcal{L}}^i = \frac{1}{N} \sum_{j=1}^N \mathcal{L}_j^i(z_j^i), \quad \bar{z}_i = \frac{1}{N} \sum_{j=1}^N z_j^i. \quad (14)$$

(4) Place $\bar{\mathcal{L}}^i$ at the mean redshift \bar{z}_i of the i -th redshift bin, now the binned flux is

$$\bar{F}(\bar{z}_i) = \bar{\mathcal{L}}^i / d_L^2(\bar{z}_i|\mathbf{s}). \quad (15)$$

The 1- σ error on each binned data point \bar{F}^i , σ_i^F , is taken to be the root mean square of the 1- σ errors on the unbinned data points in the i -th redshift bin, $\{F_j^i\}$ ($j = 1, 2, \dots, N$), multiplied by $1/\sqrt{N}$ (see Wang (2000a)).

(5) For the flux-averaged data, $\{\bar{F}(\bar{z}_i)\}$, we find

$$\chi^2 = \sum_i \frac{[\bar{F}(\bar{z}_i) - F^p(\bar{z}_i|\mathbf{s})]^2}{\sigma_{F,i}^2}, \quad (16)$$

where $F^p(\bar{z}_i|\mathbf{s}_1) = (d_L(\bar{z}_i|\mathbf{s})/\text{Mpc})^{-2}$.

⁴ Our study of intrinsic peak luminosities of nearby SNe Ia shows that their distribution is much more Gaussian in flux than in magnitude.

⁵ If the dispersions in SN Ia peak brightness were Gaussian in magnitude, flux-averaging would introduce a small bias.

⁶ Allowing both Ω_m and Ω_X to vary would lead to greatly increased uncertainty in dark energy constraints, such that no interesting constraints can be obtained from current data.

3. CONSTRAINTS ON DARK ENERGY

The Tonry/Barris SN Ia sample consists of 194 SNe Ia with $z > 0.01$ and extinction $A_V < 0.5$ (Tonry et al. 2003; Barris et al. 2003). To examine the effect of the two SNe Ia at the high redshift end ($z = 1.199$ and $z = 1.755$ respectively), we also present the results for 193 SNe Ia (omitting the SN Ia at $z = 1.755$) and 192 SNe Ia (omitting the two SNe Ia at $z = 1.199$ and $z = 1.755$).

The Knop SN Ia sample consists of 58 SNe Ia (the “All SCP SNe” data set from Knop et al. (2003)). These data should be compared with $m_B^{eff} = 5 \log(H_0 d_L) + \text{offset}$, with

$$\text{offset} = 5 \log(2997.9/h) + 25 + M_{SN}, \quad (17)$$

where M_{SN} is the peak absolute magnitude of SNe Ia. Note that for the Knop sample, the flux statistics must be done with a revised definition of flux,

$$F(z) = \left(\frac{[H_0 d_L(z)]^{data}}{\text{Mpc}} \right)^{-2} = 10^{-2(m_{eff}^B - \text{offset})/5}, \quad (18)$$

to be compared with theoretical prediction of $F^p(z|\mathbf{s}) = [H_0 d_L(z|\mathbf{s})/\text{Mpc}]^{-2}$ for a given set of cosmological parameters $\{\mathbf{s}\}$.

Note that an additional uncertainty from the redshift dispersion due to peculiar velocity must be added to the uncertainty of each SN Ia data point. The Knop sample already include a dispersion of 300 km/s along the line of site. To add 500 km/s dispersion in z to the SN data in the Tonry/Barris sample, one must propagate $\sigma_z = c^{-1} 500$ km/s into an additional uncertainty in the luminosity distance $d_L(z)$, then add it in quadrature to published uncertainty in $d_L(z)$. Note that this process is *dependent* on the cosmological model, and must be done for each set of cosmological parameters during the likelihood analysis (Riess et al. 1998; Wang 2000b).

To obtain tighter constraints on dark energy, we also include constraints from CMB (WMAP, CBI, ACBAR) and LSS (2dF) in our analysis. Since CMB data clearly indicate that we live in a flat universe, we assume $\Omega_m + \Omega_X = 1$ in all our results.⁶

We use the Markov Chain Monte Carlo (MCMC) technique (see Neil (1993) for a review), illustrated for example in Lewis & Bridle (2002), in the likelihood analysis. At its best, the MCMC method scales approximately linearly in computation time with the number of parameters. The method samples from the full posterior distribution of the parameters, and from these samples the marginalized posterior distributions of the parameters can be estimated. We have derived all our probability distribution functions (pdf) of the cosmological parameters from 10^6 MCMC samples.

3.1. The likelihood analysis

We use a χ^2 statistic

$$\chi^2 = \chi_{SN}^2 + \chi_{CMB}^2 + \chi_{LSS}^2, \quad (19)$$

where χ_{SN}^2 is given by Eq.(16) and (10) for flux statistics (with and without flux-averaging), and Eq.(9) for magnitude statistics. χ_{CMB}^2 and χ_{LSS}^2 are contributions from CMB and LSS data respectively. The likelihood $\mathcal{L} \propto e^{-\chi^2/2}$ if the measurement errors are Gaussian (Press et al. 1994).

When the cosmological parameters are varied, the shift in the whole CMB angular spectrum is determined by the shift parameter (Bond, Efstathiou, & Tegmark 1997; Melchiorri et al. 2002; Ödman et al. 2002)

$$\mathcal{R} = \sqrt{\Omega_m} H_0 r(z_{dec}) \quad (20)$$

where $r(z_{dec})$ denotes the comoving distance to the decoupling surface in a flat universe. Note that this is a robust way to include CMB constraints since the CMB depends on Ω_m and h in the combination of the physical parameter $\Omega_m h^2$. The results from CMB (WMAP, CBI, ACBAR) data correspond to $\mathcal{R}_0 = 1.716 \pm 0.062$ (using results in Spergel et al. (2003)). We include the CMB data in our analysis by adding $\chi_{CMB}^2 = [(\mathcal{R} - \mathcal{R}_0)/\sigma_{\mathcal{R}}]^2$, where \mathcal{R} is computed for each model using Eq.(20).

Following Knop et al. (2003), we include the LSS constraints from 2dF in terms of the growth parameter $f = d \ln D / d \ln a$, where a is the cosmic scale factor, and D is the linear fluctuation growth factor, $D(t) = \delta^{(1)}(\mathbf{x}, t) / \delta(\mathbf{x})$, given by

$$\ddot{D}(t) + 2H(z)\dot{D}(t) - \frac{3}{2}\Omega_m H_0^2 (1+z)^3 D(t) = 0, \quad (21)$$

where the dots denote derivatives with respect to t .

The Hubble parameter $H(z) = H_0 E(z)$ (see Eq.(2)). Since $\beta = f/b_1$, the 2dF constraints of $\beta(z \sim 0.15) = 0.49 \pm 0.09$ (Hawkins et al. 2003) and $b_1 = 1.04 \pm 0.11$ (Verde et al. 2002) yields $f_0 \equiv f(z = 0.15) = 0.51 \pm 0.11$. We include the 2dF constraints in our analysis by adding $\chi_{LSS}^2 = \{[f(z = 0.15) - f_0]/\sigma_{f_0}\}^2$, where $f = d \ln D / d \ln a$ is computed for each model using D obtained by numerically integrating Eq.(21).

Note that we have chosen to use only the most conservative and robust information, the CMB shift parameter and the LSS growth factor, from CMB and LSS observations⁷. It is important that the limits on these are independent of the assumption on dark energy made in the CMB and LSS data analysis. Further, by limiting the amount of information that we use from CMB and LSS observations to complement the SN Ia data, we minimize the effect of the systematics inherent in the CMB and LSS data on our results.

3.2. Constraints on a constant dark energy equation of state w_0

The most popular and simplest assumption about dark energy is that it has a constant equation of state w_0 . Here we present constraints on a constant dark energy equation of state.

Fig.1 shows the marginalized pdf of the matter density fraction Ω_m , the dimensionless Hubble constant h , and the constant dark energy equation of state w_0 .

The first four rows of figures in Fig.1 are results obtained using the Tonry/Barris SN Ia sample, requiring that $z > 0.01$ and extinction $A_V < 0.5$ (which yields a total of 194 SNe Ia). To examine the effect of two SNe Ia at the high redshift end ($z = 1.199$ and $z = 1.755$ respectively), we also present the results for 193 SNe Ia (omitting the SN Ia at $z = 1.755$) and 192 SNe Ia (omitting the two SNe Ia at $z = 1.199$ and $z = 1.755$). The solid, dotted, and dashed lines indicate the results for 192, 193, and 194 SNe Ia respectively.

The first two rows of figures in Fig.1 are results for SN Ia data from the Tonry/Barris sample only, without (first row) and with (second row) flux-averaging ($\Delta z = 0.05$). Note that inclusion of the two highest redshift SNe Ia at $z = 1.199$ and $z = 1.755$ leads slightly higher Ω_m and more negative w_0 . Flux-averaging leads to broader pdf for Ω_m , with somewhat lower mean Ω_m , and broader pdf for h .

The 3rd and 4th rows of figures in Fig.1 are results for SN Ia data from the Tonry/Barris sample, combined with constraints from CMB (WMAP, CBI, ACBAR) and LSS (2dF) data. The inclusion of the two highest redshift SNe Ia at $z = 1.199$ and $z = 1.755$ makes less difference in the estimated parameters, since the inclusion of the CMB and LSS data reduces the relative weight of these two data points. The main effect of flux-averaging is a broader pdf for h .

The 5th row of figures in Fig.1 are results obtained using 58 SNe Ia from the Knop sample, using flux-averaged statistics (solid) and magnitude statistics (dotted) respectively. Note flux averaging significantly broadens all the pdf's. The central figure is equivalent to a pdf in h (see Eq.(17)). These are consistent with similar results derived using the SNe Ia from the Tonry/Barris sample (3rd row of figures in Fig.1).

Table 1 gives the marginalized 68.3% and 95% confidence level (C.L.) of Ω_m , h , and w_0 . These have been computed using 10^6 MCMC samples.

3.3. Constraints on dark energy density as a free function

To place model-independent constraints on dark energy, we parametrize $\rho_X(z)$ as a continuous function, given by interpolating its amplitudes at equally spaced z values in the redshift range covered by SN Ia data ($0 \leq z \leq z_{max}$), and a constant at larger z ($z > z_{max}$, where $\rho_X(z)$ is only weakly constrained by CMB data). The values of the dimensionless dark energy density $f_i \equiv \rho(z_i)/\rho_X(0)$ ($i = 1, 2, \dots, n_f$) are the independent variables to be estimated from data. We interpolate $\rho_X(z)$ using a polynomial of order n_f for $0 \leq z \leq z_{max}$.

Since the present data can not constrain $\rho_X(z)$ for $n_f > 2$, we present results for $n_f = 2$, i.e., with $\rho_X(z)$ parametrized by its values at $z = z_{maz}/2, z_{maz}$.

Fig.2 shows the marginalized pdf of the matter density fraction Ω_m (column 1), the dimensionless Hubble constant h (column 2), and dimensionless dark energy density at $z = z_{maz}/2$ and $z = z_{maz}$ (columns 3 and 4), obtained using current SN Ia data (Tonry et al. 2003; Barris et al. 2003; Knop et al. 2003), flux-averaged and combined with

⁷ These observations provide a vast amount of information as detailed in the publications from the WMAP and 2dF teams.

CMB (WMAP, CBI, ACBAR) and 2dF data. The first three rows of figures are results for 192, 193, and 194 SNe Ia from the Tonry/Barris sample, while the fourth row are results for 58 SNe Ia from the Knop sample. The dark energy density at $z = z_{max}$ is not well constrained when the $z = 1.755$ SN Ia is included in the analysis; this is as expected since this extends $\rho_X(z)$ to $z_{max} = 1.755$, with only one SN Ia at $z > 1.2$.

Note that when the estimated parameters are well constrained, flux averaging generally leads to slightly lower estimates of Ω_m and $\rho_X(z)$ (at $z = z_{max}/2$ and $z = z_{max}$).

Table 2 gives the marginalized 68.3% and 95% C.L. of Ω_m , h , $\rho_X(z_{max}/2)/\rho_X(0)$, and $\rho_X(z_{max})/\rho_X(0)$. These have been computed using 10^6 MCMC samples.

Fig.3 shows the dark energy density $\rho_X(z)$ reconstructed from current SN Ia (the Tonry/Barris sample and the Knop sample), CMB (WMAP, CBI, ACBAR) and LSS (2dF) data. The heavy (light) lines indicate the 68.3% (95%) C.L. of the reconstructed $\rho_X(z)$. The dot-dashed line indicates the cosmological constant model, $\rho_X(z)/\rho_X(0) = 1$. The 68.3% and 95% C.L.'s of $\rho_X(z)$ are marginalized confidence levels, computed at each z using 10^6 MCMC samples, with the correlation between $\rho_X(.5z_{max})$ and $\rho_X(z_{max})$ fully included.

Fig.3(a) shows the reconstructed $\rho_X(z)$ using 192, 193, and 194 SNe Ia from the Tonry/Barris sample, flux-averaged and combined with CMB (WMAP, CBI, ACBAR) and LSS (2dF) data. The densely (sparsely) shaded regions are the 68.3% (95%) C.L. of $\rho_X(z)$ for 192 SNe Ia (at $z \leq 1.056$). The heavy (light) dotted and dashed lines are the 68.3% (95%) C.L. of $\rho_X(z)$ for 193 and 194 SNe Ia respectively. Note that the $\rho_X(z)$ reconstructed from 193 SNe Ia (adding the SN Ia at $z = 1.199$) nearly overlaps from that from 192 SNe Ia for $z \lesssim 1.056$. However, the $\rho_X(z)$ reconstructed from 194 SNe Ia (adding the SNe Ia at $z = 1.199$ and $z = 1.755$) deviates notably from that from 192 SNe Ia for $0.7 \lesssim z \lesssim 1.056$, although the 68.3% C.L. regions overlap. Clearly, the reconstructed $\rho_X(z)$ is constant for $0 \lesssim z \lesssim 0.5$ and increases with redshift z for $0.5 \lesssim z \lesssim 1$ at 68.3% C.L., but is consistent with a constant at 95% C.L. We note that at 90% C.L., $\rho_X(.5z_{max})/\rho(0) = [0.83, 1.59]$, and $\rho_X(z_{max})/\rho(0) = [1.03, 6.85]$; this indicates that $\rho_X(z)$ varies with time at approximately 90% C.L.

Fig.3(b) shows the reconstructed $\rho_X(z)$ using 192 SNe Ia from the Tonry/Barris sample (same as in Fig.3(a)) and that from the 58 SNe Ia of the Knop sample (dotted lines). The 68.3% C.L. regions overlap. However, the 58 SCP SNe Ia seem to favor $\rho_X(z) \lesssim 1$ at $0.5 \lesssim z \lesssim 1$, and has much larger uncertainties at $z \gtrsim 0.5$.

3.4. Comparison with previous work

The SN observational teams have published their data together with constraints on a constant dark energy equation of state (Tonry et al. 2003; Knop et al. 2003). These results should be compared with our results for a constant $w_X(z)$ using magnitude statistics (see Table 1). Using a 2dF prior of $\Omega_m h = 0.20 \pm 0.03$ (Percival et al. 2002) and assuming a flat universe, Tonry et al. (2003) found that $-1.48 < w_0 < -0.72$ at 95% C.L.; this is close to $-1.24 < w_0 < -0.74$ at 95% C.L. (using 192 SNe Ia together with CMB and LSS constraints as discussed in

Sec.3.1) from Table 1. Using the same CMB and LSS constraints as us and assuming a flat universe, Knop et al. (2003) found that $w_0 = -1.05^{+0.15}_{-0.20}$ (statistical) ± 0.09 (identified systematics) at 68.3% C.L.; close to our results of $w_0 = -0.99 \pm 0.16$ at 68.3% C.L.

At the completion of our analysis, we became aware that Alam et al. (2003) and Choudhury & Padmanabhan (2003) have found that current SN Ia data favor $w_X(z) < -1$. Although our results are qualitatively consistent with these, there are significant differences in both analysis technique and quantitative results.

Alam et al. (2003) used 172 SNe Ia from Tonry et al. (2003), and obtained a reconstructed $w_X(z)$ that deviates quite significantly from $w_X(z) = -1$. In their paper (v2), Figs.3 and 14 (both assuming $\Omega_m = 0.3$) are consistent with what we found. We note that some of their reconstructed $w_X(z)$'s (see their Figs.4, 6, 8, 10, and 16) have decreasing errors for $z \gtrsim 1.2$ (where there are only two SNe Ia). This illustrates the fact that while free fitting forms for $\rho_X(z)$ or $w_X(z)$ generally give increasing errors with redshift (large error where there are very few observed SNe Ia, see Fig.3 of this paper), this may not be true for other parametrizations (such as used in Alam et al. (2003)).

Choudhury & Padmanabhan (2003) used 194 SNe Ia (the Tonry/Barris sample), and presented their results for $w_X(z) = w_0 + w_1 z/(1+z)$ with $\Omega_m = 0.29, 0.34$, and 0.39 (no marginalization over Ω_m).

4. SUMMARY AND DISCUSSION

In order to place model-independent constraints on dark energy, we have reconstructed the dark energy density $\rho_X(z)$ as a free function from current SN Ia data (Tonry et al. 2003; Barris et al. 2003; Knop et al. 2003), together with CMB (WMAP, CBI, and ACBAR) and LSS (2dF) data. We find that the dark energy density $\rho_X(z)$ is constant for $0 \lesssim z \lesssim 0.5$ and increases with redshift z for $0.5 \lesssim z \lesssim 1$ at 68.3% C.L., but is consistent with a constant at 95% C.L. (see Fig.3).

Flux-averaging of SN Ia data is required to yield cosmological parameter constraints that are free of the bias induced by weak gravitational lensing (Wang 2000b). We have developed a consistent framework for flux-averaging analysis of SN Ia data, and applied it to current SN Ia data. We find that flux-averaging of SN Ia data generally leads to slightly lower Ω_m and smaller time-variation in $\rho_X(z)$.

We note that flux-averaging of SNe Ia has more effect on the Knop sample than the Tonry/Barris sample. This may be due to the fact that the measurement errors of the majority of the SNe Ia in the Tonry/Barris sample have been ‘‘Gaussianized’’ in magnitudes by averaging over several different analysis techniques (Tonry et al. 2003). However, it is likely that SN Ia peak brightness distribution is Gaussian in *flux*, instead of magnitudes (Wang et al. 2004). A consistent framework for flux-averaging is only straightforward (as presented in Sec.2) if the distribution of SN Ia peak brightnesses is Gaussian in flux. Our results suggest that observers should publish observed SN Ia peak brightnesses with uncertainties in flux, to allow detailed flux-averaging studies.

Our results include an estimate of the Hubble constant $H_0 = h 100 \text{ km/s Mpc}^{-1}$ from the Tonry/Barris sample of

194 SNe Ia. Since the Tonry/Barris sample data used a fixed value of $h_{fix} = 0.65$ (Tonry et al. 2003) in the derived distances, we divide their derived distances $H_0 d_L(z)$ by h_{fix} and marginalize over H_0 in our analysis. Our MCMC method yields smooth pdf's for all marginalized parameters. The errors on the estimated h in Tables 1 & 2 are statistical errors only, not including a much larger systematic error contributed by the intrinsic dispersion in SN Ia peak luminosity of $\sigma_m^{int} \simeq 0.17$ magnitudes Hamuy et al. (1996). This implies a systematic uncertainty in h of 7.83%, or $\sigma_h^{int} \simeq 0.05$ for the h values tabulated in Table 1 & 2. This yields an estimate for h that overlap with those from Branch (1998) and Freedman et al. (2001) within 1σ .

It is intriguing that the current SN Ia data, together with CMB and galaxy survey data, indicate that $\rho_X(z)$

varies with time at approximately 90% C.L. (see Fig.3 and Sec.3.3). If the trend in $\rho_X(z)$ that we have found is confirmed by future observational data, it will have revolutionary implications for particle physics and cosmology. Since the uncertainty in $\rho_X(z)$ is large where there are few observed SNe Ia (see Fig.3), we expect that a significant increase in the number of SNe Ia, obtained from dedicated deep SN Ia searches (Wang 2000a), will allow us to place robust and more stringent constraints on the time-dependence of the dark energy density.

This work is supported in part by NSF CAREER grant AST-0094335. We are grateful to David Branch and Michael Vogeley for helpful comments.

REFERENCES

- Aguirre, A.N. 1999, ApJ, 512, L19
 Alam, U.; Sahni, V.; Saini, T.D.; & Starobinsky, A.A. 2003, astro-ph/0311364
 Albrecht, A.; Burgess, C.P.; Ravndal, F.; & Skordis, C. 2002, Phys. Rev. D65, 123507
 Armendariz-Picon, C., Mukhanov, V., Steinhardt, P.J. 2000, Phys. Rev. Lett. 85, 4438
 Barger, V., & Marfatia, D. 2001, Phys. Lett. B, 498, 67
 Barris, B.J., et al. 2003, astro-ph/0310843, ApJ, in press
 Bean, R.; & Melchiorri, A. 2002, Phys. Rev. D65, 041302
 Bennett, C., et al. 2003, ApJ, Suppl. 148, 1
 Bernstein, G.M.; & Jain, B. 2003, astro-ph/0309332, ApJ, in press
 Bond, J.R.; Efstathiou, G.; & Tegmark, M. 1997, MNRAS, 291, L33
 Boyle, L.A.; Caldwell, R.R.; Kamionkowski, M. 2002, Phys. Lett. B545, 17
 Branch, D. 1998, ARA&A, 36, 17
 Caldwell, R., Dave, R., Steinhardt, P. 1998, Phys. Rev. Lett., 80, 1582
 Carroll, S.M.; Hoffman, M., & Trodden, M. 2003, Phys. Rev. D68, 023509
 Choudhury, T.R., & Padmanabhan, T. 2003, astro-ph/0311622
 Daly, R.A., & Djorgovski, S.G. 2003, ApJ, 597, 9
 Deffayet, C. 2001, Phys. Lett. B502, 199
 Dodelson, S., Kaplinghat, M., & Stewart, E. 2000, Phys. Rev. Lett. 85, 5276
 Drell, P.S.; Lored, T.J.; & Wasserman, I. 2000, ApJ, 530, 593
 Farrar, G.R., & Peebles, P. J. E. 2003, astro-ph/0307316
 Freedman, W. L. et al. 2001, ApJ, 553, 47
 Freese, K., Adams, F.C., Frieman, J.A., and Mottola, E. 1987, Nucl. Phys. B287, 797
 Freese, K., and Lewis, M., 2002, Phys. Lett., B540, 1
 Frieman, J., Hill, J., Stebbins, A., and Waga, I. 1995, Phys. Rev. Lett., 75, 2077
 Frieman, J. A. 1997, Comments Astrophys., 18, 323
 Gerke, B.F., Efstathiou, G. 2002, MNRAS, 335, 33
 Griest, K. 2002, Phys. Rev. D66, 123501
 Hamuy, M., et al. 1996, AJ, 112, 2408
 Hannestad, S., & Mortsell, E. 2002, Phys. Rev. D66, 063508
 Hawkins, E. et al. 2003, astro-ph/0212375, MNRAS in press
 Holz, D.E. & Wald, R.M. 1998, Phys. Rev., D58, 063501
 Hu, W. 2002, Phys.Rev. D66, 08351
 Huterer, D., Ma, C. 2003, astro-ph/0307301
 Huterer, D., & Turner, M.S. Phys. Rev. D64, 123527
 Jimenez, R. 2003, New Astron. Rev. 47, 761
 Kantowski, R.; Vaughan, T.; Branch, D. 1995, ApJ, 447, 35
 Knop, R. A., et al. 2003, astro-ph/0309368, ApJ, in press
 Kujat, J.; Linn, A.M.; Scherrer, R.J.; & Weinberg, D.H. 2002, ApJ, 572, 1
 Kuo, C.L., et al. 2002, submitted to ApJ, astro-ph/0212289
 Lewis, A., & Bridle, S. 2002, Phys. Rev. D, 66, 103511, astro-ph/0205436
 Maor, I., Brustein, R., & Steinhardt, P.J. 2001, Phys. Rev. Lett., 86, 6; Erratum-ibid. 87 (2001) 049901
 Maor, I.; Brustein, R.; McMahon, J.; & Steinhardt, P.J. 2002, Phys. Rev. D65, 123003
 Melchiorri, A.; Mersini, L.; Ödman, C.J.; & Trodden, M. 2002, astro-ph/0211522
 Metcalf, R. B., & Silk, J. 1999, ApJ, 519, L1
 Majumdar, S., & Mohr, J.J. 2003, astro-ph/0305341, submitted to ApJ
 Mukherjee, P.; Banday, A.J.; Riazuelo, A.; Gorski, K.M.; & Ratra, B. 2003, astro-ph/0306147, ApJ, in press
 Munshi, D.; Porciani, C.; & Wang, Y. 2003, astro-ph/0302510, MNRAS, in press
 Munshi, D., and Wang, Y. 2003, ApJ, 583, 566
 Neil, R.M. 1993, ftp://ftp.cs.utoronto.ca/pub/radford/review.ps.gz
 Ödman, C.J.; Melchiorri, A.; Hobson, M.P.; & Lasenby, A.N. 2002, astro-ph/0207286
 Padmanabhan, T. 2003, Physics Reports 380, 235-320
 Peebles, P. J. E.; Ratra, B. 1988, ApJ, 325L, 17
 Peebles, P. J. E.; Ratra, B. 2003, Rev.Mod.Phys. 75, 559-606
 Pearson, T.J., et al. 2003, ApJ, 591, 556-574
 Percival, W.J. et al. 2002, MNRAS, 337, 1068
 Perlmutter, S., et al. 1999, ApJ, 517, 565
 Phillips, M.M., ApJ, 413, L105 (1993)
 Podariu, S.; & Ratra, B. 2001, ApJ, 563, 28
 Press, W.H., Teukolsky, S.A., Vetterling, W.T., & Flannery, B.P. 1994, Numerical Recipes, Cambridge University Press, Cambridge.
 Riess, A. G., et al. 1998, AJ, 116, 1009
 Riess, A.G., Press, W.H., and Kirshner, R.P., ApJ, 438, L17 (1995)
 Riess, A.G., et al. 1999, AJ, 118, 2675
 Sahni, V., & Shtanov, Y. 2002, astro-ph/0202346
 Schulz, A.E.; & White, M. 2001, Phys. Rev. D64, 043514
 Seo, H.; & Eisenstein, D.J. 2003, astro-ph/0307460
 Sereno, M. 2002, Astron. Astrophys., 393, 757
 Spergel, D.N., et al. 2003, astro-ph/0302209
 Tegmark, M. 2002, Phys. Rev. D66, 103507
 Tonry, J.L., et al. 2003, ApJ, 594, 1-24
 Verde, L. et al. 2002, MNRAS, 335, 432
 Viel, M.; Matarrese, S.; Theuns, T.; Munshi, D.; & Wang, Y. 2003, MNRAS, 340, L47
 Wambsganss, J., Cen, R., Xu, G., & Ostriker, J.P. 1997, ApJ, 475, L81
 Wang, Y. 1999, ApJ, 525, 651
 Wang, Y. 2000a, ApJ, 531, 676
 Wang, Y. 2000b, ApJ, 536, 531
 Wang, Y., and Garnavich, P. 2001, ApJ, 552, 445
 Wang, Y., and Lovelace, G. 2001, ApJ, 562, L115
 Wang, Y., Holz, D.E., and Munshi, D. 2002, ApJ, 572, L15
 Wang, Y.; Freese, K.; Gondolo, P.; & Lewis, M. 2003, ApJ, 594, 25
 Wang, Y., et al. 2004, in preparation
 Wasserman, I. 2002, Phys. Rev. D66, 123511
 Weller, J., & Lewis, A.M. 2003, MNRAS, in press
 Zhu, Z.; & Fujimoto, M. 2003, astro-ph/0312022, ApJ in press

Table 1

Estimated cosmological parameters (mean, 68.3% C.L., 95% C.L.) assuming $w_X(z) = w_0$

Tonry/Barris sample SNe		Ω_m	h^a	w_0	χ^2_{min}/N^c_{dof}
192 SNe ($z_{max}=1.056$)					
flux, binned ^b		.47 [.36, .57][.14, .63]	.661 [.645, .674][.631, .690]	-2.37 [-3.56, -1.20][-5.34, -.69]	13.34/19
flux, unbinned		.47 [.43, .52][.34, .55]	.656 [.644, .666][.636, .676]	-3.08 [-4.09, -2.08][-5.50, -1.46]	209.10/189
mag.; unbinned		.49 [.41, .57][.22, .61]	.662 [.651, .671][.644, .681]	-2.25 [-3.18, -1.34][-4.36, -.80]	193.36/189
193 SNe ($z_{max}=1.199$)					
flux, binned ^b		.48 [.39, .58][.18, .63]	.661 [.645, .676][.631, .690]	-2.53 [-3.85, -1.30][-5.54, -.73]	14.36/20
flux, unbinned		.48 [.43, .52][.35, .56]	.656 [.645, .665][.637, .676]	-3.13 [-4.10, -2.13][-5.64, -1.50]	210.56/190
mag.; unbinned		.51 [.44, .58][.29, .62]	.663 [.653, .671][.644, .683]	-2.47 [-3.42, -1.49][-5.14, -.91]	194.86/190
194 SNe ($z_{max}=1.755$)					
flux, binned ^b		.49 [.40, .58][.20, .63]	.661 [.645, .675][.632, .690]	-2.54 [-3.80, -1.34][-5.62, -.76]	14.40/21
flux, unbinned		.48 [.44, .52][.37, .56]	.656 [.645, .665][.637, .675]	-3.17 [-4.13, -2.22][-5.47, -1.58]	210.74/191
mag.; unbinned		.51 [.45, .58][.30, .62]	.663 [.653, .671][.644, .683]	-2.51 [-3.46, -1.55][-4.97, -.95]	194.88/191
192 SNe ($z_{max}=1.056$) + CMB & LSS					
flux, binned ^b		.28 [.23, .33][.19, .39]	.652 [.638, .665][.627, .677]	-.95 [-1.09, -.82][-1.27, -.72]	15.44/21
flux, unbinned		.26 [.22, .31][.18, .36]	.643 [.634, .650][.627, .657]	-1.15 [-1.29, -1.00][-1.53, -.90]	216.76/191
mag.; unbinned		.29 [.24, .34][.21, .39]	.654 [.646, .661][.639, .668]	-.95 [-1.07, -.83][-1.24, -.74]	196.60/191
193 SNe ($z_{max}=1.199$) + CMB & LSS					
flux, binned ^b		.29 [.24, .34][.20, .39]	.652 [.638, .663][.626, .676]	-.95 [-1.08, -.82][-1.27, -.71]	17.04/22
flux, unbinned		.27 [.22, .31][.18, .37]	.643 [.635, .650][.627, .658]	-1.15 [-1.29, -1.00][-1.54, -.90]	219.00/192
mag.; unbinned		.30 [.25, .35][.21, .40]	.654 [.645, .660][.638, .667]	-.95 [-1.07, -.82][-1.25, -.74]	199.04/192
194 SNe ($z_{max}=1.755$) + CMB & LSS					
flux, binned ^b		.29 [.24, .34][.20, .40]	.651 [.638, .663][.625, .676]	-.95 [-1.08, -.81][-1.28, -.71]	17.44/23
flux, unbinned		.27 [.22, .32][.18, .37]	.642 [.634, .650][.627, .657]	-1.15 [-1.31, -1.00][-1.57, -.90]	219.8/193
mag.; unbinned		.30 [.25, .35][.21, .41]	.654 [.645, .660][.638, .668]	-.95 [-1.07, -.82][-1.27, -.73]	199.50/193
58 Knop sample SNe ($z_{max}=0.863$) + CMB & LSS					
		Ω_m	offset-23.5	w_0	χ^2_{min}/N^c_{dof}
flux, binned ^b		.22 [.15, .28][.11, .36]	.414 [.347, .480][.286, .547]	-1.20 [-1.45, -.96][-1.73, -.74]	9.1/13
flux, unbinned		.21 [.16, .26][.13, .32]	.395 [.356, .434][.321, .471]	-1.18 [-1.34, -1.02][-1.54, -.88]	61.34/57
mag.; unbinned		.27 [.21, .32][.17, .39]	.367 [.331, .406][.295, .441]	-.99 [-1.15, -.83][-1.34, -.70]	55.86/57

^a Statistical error only, not including the contribution from the much larger SN Ia absolute magnitude error of $\sigma_h^{int} \simeq 0.05$ (see Sec.4).

^b Flux-averaged with $\Delta z = .05$. ^c The number of degrees of freedom.

Table 2

Estimated cosmological parameters (mean, 68.3% C.L., 95% C.L.) for arbitrary $\rho_X(z)$, from SN Ia data combined with CMB and LSS data

	Ω_m	h^a	$\rho_X(.5 z_{max})/\rho_X(0)$	$\rho_X(z_{max})/\rho_X(0)$	χ^2_{min}/N^c_{dof}
Tonry/Barris sample					
192 SNe ($z_{max}=1.056$)					
binned flux ^b	.33 [.27, .39][.22, .46]	.660 [.644, .673][.630, .688]	1.19 [.97, 1.42][.76, 1.67]	3.61 [1.84, 5.41][.73, 7.53]	13.28/20
unbinned flux	.34 [.28, .39][.24, .45]	.655 [.645, .663][.637, .671]	1.09 [.88, 1.31][.67, 1.56]	5.02 [3.27, 6.82][1.98, 9.15]	208.26/190
unbinned mag.	.34 [.28, .40][.23, .46]	.662 [.652, .670][.645, .678]	1.22 [1.01, 1.43][.80, 1.66]	3.75 [2.05, 5.40][.94, 7.76]	193.30/190
193 SNe ($z_{max}=1.199$)					
binned flux ^b	.35 [.28, .41][.23, .48]	.660 [.645, .674][.631, .688]	1.39 [1.08, 1.69][.84, 2.10]	4.95 [2.55, 7.34][.88, 10.35]	14.24/21
unbinned flux	.36 [.30, .42][.25, .49]	.656 [.645, .664][.637, .672]	1.44 [1.06, 1.82][.80, 2.41]	7.50 [4.39, 10.69][2.57, 15.57]	209.42/191
unbinned mag.	.36 [.30, .42][.25, .48]	.662 [.653, .670][.645, .678]	1.42 [1.13, 1.71][.89, 2.08]	5.14 [2.88, 7.43][1.41, 10.62]	194.50/191
194 SNe ($z_{max}=1.755$)					
binned flux ^b	.40 [.32, .48][.25, .54]	.661 [.646, .675][.632, .688]	3.26 [1.76, 4.76][1.02, 5.75]	15.64 [6.22, 25.30][.92, 30.53]	14.5/22
unbinned flux	.38 [.32, .43][.27, .48]	.654 [.644, .662][.637, .670]	2.85 [1.88, 3.81][1.18, 4.69]	14.78 [8.77, 20.58][4.36, 25.83]	209.88/192
unbinned mag.	.38 [.31, .44][.26, .50]	.662 [.652, .669][.645, .678]	2.48 [1.66, 3.54][1.22, 4.35]	10.60 [5.41, 17.81][2.68, 21.80]	194.70/192
Knop sample					
58 SNe ($z_{max}=0.863$)					
	Ω_m	offset-23.5	$\rho_X(.5 z_{max})/\rho(0)$	$\rho_X(z_{max})/\rho(0)$	χ^2_{min}/N^c_{dof}
binned flux ^b	.34 [.25, .43][.18, .52]	.311 [.210, .409][.127, .509]	.91 [.59, 1.22][.38, 1.61]	5.92 [2.13, 9.73][.58, 13.21]	7.2/12
unbinned flux	.26 [.18, .33][.12, .41]	.381 [.331, .428][.286, .474]	.85 [.67, 1.03][.50, 1.21]	1.96 [.53, 3.55][.09, 5.45]	61.32/56
unbinned mag.	.39 [.30, .48][.22, .56]	.309 [.256, .362][.208, .412]	1.18 [.89, 1.46][.67, 1.82]	6.10 [2.47, 9.59][.86, 12.57]	53.90/56

^a Statistical error only, not including the contribution from the much larger SN Ia absolute magnitude error of $\sigma_h^{int} \simeq 0.05$ (see Sec.4).

^b flux-averaged with $\Delta z = .05$. ^c The number of degrees of freedom.

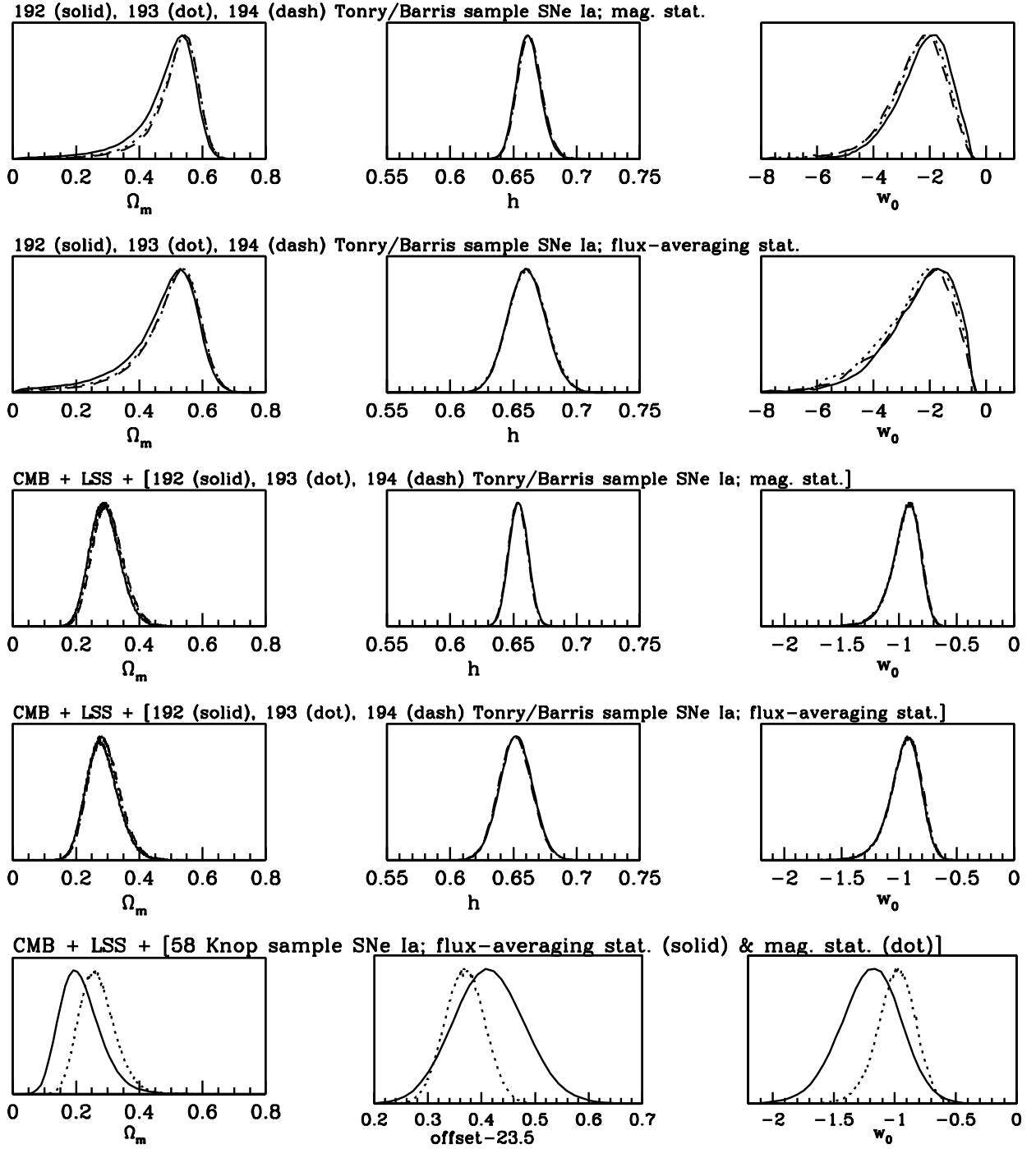


FIG. 1.— The marginalized probability distributions of Ω_m , h , and the constant equation of state for the dark energy w_0 .

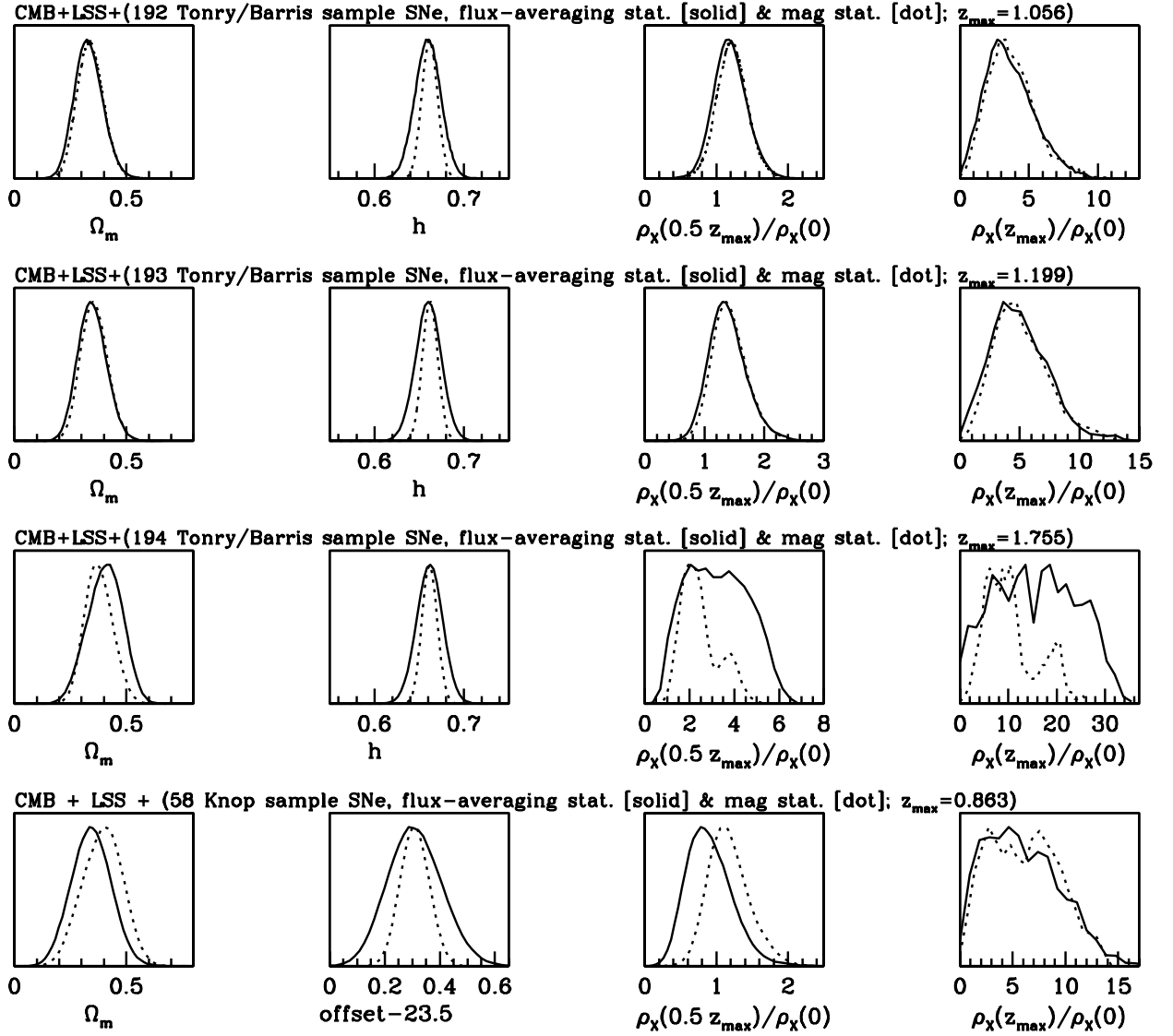


FIG. 2.— The marginalized probability distributions of Ω_m , h , and dimensionless dark energy density at $z = z_{\max}/2$ and $z = z_{\max}$.

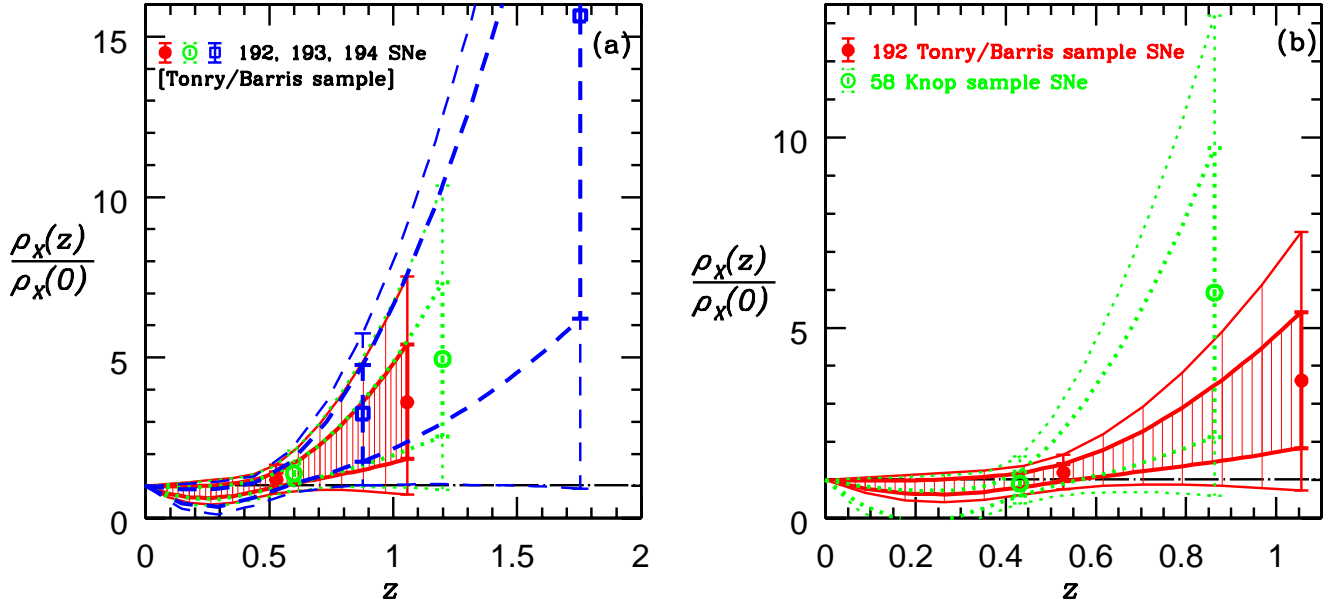


FIG. 3.— The dark energy density $\rho_X(z)$ reconstructed from current SN Ia (Tonry/Barris sample and Knop sample), CMB (WMAP, CBI, ACBAR), and LSS (2dF) data. The densely (sparsely) shaded regions are the 68.3% (95%) C.L. of $\rho_X(z)$ for 192 Tonry/Barris sample SNe Ia (at $z \leq 1.056$). The heavy (light) lines indicate the 68.3% (95%) C.L. of the reconstructed $\rho_X(z)$. The dot-dashed line indicates the cosmological constant model, $\rho_X(z)/\rho_X(0) = 1$. (a) Reconstructed $\rho_X(z)$ using 192 (shaded regions), 193 (dotted lines), and 194 (dashed lines) SNe Ia from the Tonry/Barris sample (Tonry et al. 2003; Barris et al. 2003). (b) Reconstructed $\rho_X(z)$ using 192 Tonry/Barris sample SNe Ia (shaded regions) and 58 Knop sample SNe Ia (dotted lines) (Knop et al. 2003).